

# Nanotechnology Driven Approach with Collagen and Mupirocin-loaded Silver Nanoparticles in Chitosan Hydrogel for Burn Wound Infection

K. Priyadharshini, Veinramuthu Sankar

Department of Pharmaceutics, PSG College of Pharmacy, Coimbatore, Tamil Nadu, India

## Abstract

**Aim:** The present investigation was to formulate Mupirocin- and collagen-loaded silver nanoparticles in chitosan hydrogel which has synergistic wound healing and anti-bacterial activity. **Materials and Methods:** Extraction and characterization of acid-soluble collagen from tilapia fish scales were performed. Mupirocin and collagen silver nanoparticles (Mup-AgNP-Col) were synthesized by chemical reduction method using sodium borohydride as reducing agent. Using design expert software, Mup-AgNP-Col preparations were optimized. Chitosan hydrogel was prepared and the optimized Mup-AgNP-Col formulation was loaded in the gel and evaluation parameters were assessed. **Results:** The optimized Mup-AgNP-Col formulation with silver nitrate concentrations of 4.3 mM, sodium borohydride concentration of 2 mM, and collagen concentration of 0.1 mg showed spherical structure with particle size as  $121 \pm 1.18$  nm. The entrapment efficiency was found to be  $91.3 \pm 2.8$  % and at the end of 6 h *in vitro*, release studies showed  $91 \pm 2.89$  % drug release in phosphate buffer, pH 7.4. Non-toxic and wound-healing activity was confirmed by L929 fibroblast cell line study. The formulated gel was evaluated for its spreadability and extrudability. **Conclusion:** Mup-AgNP-Col in chitosan hydrogel enhances burn wound healing.

**Key words:** Burn wound infection, chitosan, collagen, silver nanoparticles

## INTRODUCTION

The rate of burns is higher in adults than in children and the effect is known to be potentially fatal. Sepsis continues to be the leading cause of death despite a variety of current topical therapy plans intended to eliminate the bacterial burden within the burn wound.<sup>[1]</sup> Due to their superior chemical stability and confined surface plasma resonance, silver nanoparticles are gaining more knowledge in the field of medicine. AgNPs have a broad antibacterial spectrum, so it is believed that they might have a great deal of potential to speed up wound healing in burn wound infections.<sup>[2]</sup>

The protein collagen has been used to treat burn wound infections. Collagen has a high level of biocompatibility, low allergenicity, and antigenicity. It works synergistically with bioactive components and is bioabsorbable, hemostatic, biodegradable, non-toxic, and also compatible with both natural and synthetic polymers. It has a strong affinity for water molecules and good tensile strength.<sup>[3]</sup>

A natural antibiotic Mupirocin, formerly known as pseudomonic acid, is prepared through the submerged fermentation of *Pseudomonas fluorescens*. Mupirocin is a topical medication that has been used in burns to treat multidrug-resistant bacteria and wound infections caused by burns.<sup>[4]</sup>

The intrinsic antimicrobial capabilities and capacity to efficiently transfer extrinsic antimicrobial chemicals into the affected area, the cationic natural polymer chitosan has received extensive research attention as an antimicrobial agent for preventing and treating infections.<sup>[5]</sup> Chitosan hydrogels can be used as a multifunctional wound dressing to cover wounds, manage wound infections, and promote healing by delivering anti-bacterial materials.<sup>[6]</sup>

**Address for correspondence:** Dr. Veinramuthu Sankar, Department of Pharmaceutics, PSG College of Pharmacy, Coimbatore, Tamil Nadu, India. Phone: +91-9486220270. E-mail: sansunv@yahoo.co.in

**Received:** 03-04-2023

**Revised:** 17-06-2023

**Accepted:** 24-06-2023

In this study, we formulated silver nanoparticle formulation with collagen and Mupirocin in hydrogel for treating burn wound infection and antimicrobial and Methicillin resistance *Staphylococcus aureus* (MRSA) activity were evaluated.

## MATERIALS AND METHODS

### Materials

Mupirocin was a gifted sample from Fourts (India) Laboratories Pvt. Limited, Chennai. Silver nitrate-Sigma aldrich, Sodium borohydride-Sigma aldrich, Glacialacetic acid-Loba chemie Pvt Ltd, Mumbai and Chitosan-Sigma aldrich.

### Methods

#### Extraction of collagen from fish scales

Tilapia scales (*Oreochromis niloticus*) were removed, washed with water, and then treated with 0.1 mol/L NaHCO<sub>3</sub> for 6 h to remove non-collagenous proteins followed by neutralizing it with water. The scales were cut into small pieces and subjected to acid-soluble collagen (ASC) extraction by treating with 0.5 mol/L acetic acid for 24 h. The residue was collected after centrifuging at 10,000 RPM for 20 min and dissolved in 0.5 mol/L acetic acid at the ratio of 1:9 (w/v) and then dialyzed in 0.1 mol/L acetic acid, followed by distilled water. All processes were carried out at 4°C and then lyophilized.<sup>[7]</sup>

### Characterization of collagen

#### Collagen yield

The yield of ASC was calculated based on the weight of the lyophilized sample by dry weight of the starting material.<sup>[7]</sup>

#### Melting point

The melting point of collagen was determined using capillary tube method.

#### UV-visible spectroscopy

For the determination of lambda max of collagen, it was solubilized in acetic acid 0.5 M and analyzed spectrometrically.

#### SEM analysis

The lyophilized collagen sample was cut using a punch and fixed to a glass slide and the excess water was made to evaporate in room temperature for 24 h. Gold coating was done under vacuum and then analyzed under accelerating voltage of 15–20 kV.<sup>[8]</sup>

#### Fourier transform infrared (FTIR) spectroscopic analysis

FTIR spectra of the collagen sample were derived using FTIR spectrometer.<sup>[7]</sup>

### DoE for silver nanoparticles optimization

For statistical optimization of formulation, 2<sup>3</sup> factorial designs were used. Silver nitrate, sodium borohydride, and collagen were the independent variables at two different levels. The dependent variables are size of the particles (Y1), entrapment efficiency (Y2), and % drug release (Y3). The performing values were fed into a Design Expert software and anatomized.<sup>[9]</sup>

### Synthesis of silver nanoparticles, along with collagen

Silver nanoparticles were synthesized by chemical reduction method using sodium borohydride as reducing agent. Silver nitrate at a concentration of 4.3 mM solution was prepared. Collagen at a concentration of 0.1 mg/mL was prepared by dissolving in 0.5 M acetic acid solution, homogenized for 10 min at 15,000 rpm, and centrifuged at 3600 rpm for 15 min maintained at temperature 25°C. Then, the solution was added to the silver nitrate solution and agitated in a magnetic stirrer. Sodium borohydride at a concentration of 2 mM solution was added drop-wise to the silver salt solution. Finally, the color of the mixture slowly turns from colorless to yellow indicating the reduction of Ag<sup>+</sup> ions.<sup>[3,10]</sup>

### Loading of Mupirocin on AgNP-Col

Mupirocin is loaded to AgNP-Col by electrostatic interaction method by forming a bond between two oppositely charged particles. 40 mg of Mupirocin was added to 40 mL (1mg/ml) of AgNP-Colsolution and gently stirred in a magnetic stirrer at room temperature for 24 h. UV Visible spectroscopy was used to confirm the formulation spectrum.

### UV spectrophotometric analysis

To evaluate the reduction of silver ions in the solution, the surface plasmon resonance (SPR) of Mup-AgNP-col formulation was measured, and the  $\lambda_{max}$  was scanned in the wavelength range of 300–800 nm using a glass cuvette with pure water as blank in UV visible spectrophotometer.<sup>[11]</sup>

### Characterization of Mup-AgNP-Col

#### Dynamic light scattering (DLS)

DLS was used to determine the mean particle size diameter, Polydispersity index, and Zeta potential (Nano ZS 90, Malvern Instruments).

#### Entrapment efficiency

About 2ml of Mup-AgNP-Col was taken in an eppendorf tube and centrifuged at 13,000 rpm for 15 min at 4°C and 1 mL of the supernatant was collected, diluted, and analyzed in UV visible spectrophotometer at 222 nm and then the amount of drug entrapped and entrapment efficiency was calculated.<sup>[11]</sup>

### ***In vitro release studies***

About 2 mL of the Mup-AgNP-Col liquid formulation was taken in a dialysis bag and placed in a beaker containing 200 mL phosphate buffer pH 7.4 at room temperature and allowed to stir gently at 100 rpm using magnetic stirrer. Samples were withdrawn at periodic time intervals from 1 h to 6 h and replaced with equal volume of buffer and analyzed spectrometrically at 222 nm after making suitable dilutions.<sup>[11]</sup>

### ***Atomic force microscopy***

AFM was used to determine the surface morphology, roughness, and diameter of nanoparticles. The sample was taken on a glass stubby by pouring a very little amount of nanoparticulate formulation (5  $\mu$ L) onto it and then analyzing the picture.<sup>[12]</sup>

### ***Compatibility studies***

FTIR studies were carried out for physical mixtures of the formulation by KBr press pellet technique.<sup>[11]</sup>

### ***Zone of inhibition test by disc diffusion assay***

Muller-Hinton (MH) agar medium was prepared and autoclaved for 20 min. *S. aureus* and MRSA bacterial species were chosen. A cotton swab was dipped in the bacterial suspension containing *S. aureus* and MRSA, wiped over the surface of the MH agar plates to inoculate the bacteria. The disc diffusion method was used to test the antimicrobial activity of Mupirocin, AgNP-Col, and Mup-AgNP-Col formulations against the *S. aureus* and MRSA strain. Equivalent quantity of formulation was placed on a separate sterile disc and dried. As a positive control, 10  $\mu$ g of Ciprofloxacin was employed. The bacterial Petri dish was then cultured for 24 h at 37°C. A clear zone around the disc reveals the susceptibility of the test organism and the diameter of the inhibited zone was also assessed.<sup>[13]</sup>

### ***In vitro scratch assay***

Scratch assay was carried out to observe the wound-healing activity of the formulation in L929 fibroblast cell lines. The cells were pretreated with phosphate buffer and then immediately cultured with the Mup-AgNP-Col formulations and 0.2% PBS was kept as control. The cells were incubated at 37°C for 24 h and the image was observed under phase contrast microscope at 0 h, 4 h, 18 h, and 24 h.<sup>[14]</sup>

### ***In vitro cytotoxicity study***

*In vitro* cytotoxicity study was performed to analyze the cytotoxicity effect on L929 cells. It is a colorimetric assay based on the reduction of yellow-colored water-soluble tetrazolium dye MTT to formazan crystals. Different concentrations of the sample Mup-AgNP-Col at 6.25, 12.5, 25, 50, 100, and 200  $\mu$ g/ml were incubated for 24 h at 37°C in a 5% CO<sub>2</sub> atmosphere and MTT reagent was added and

incubated for 3 h. Then, 100  $\mu$ L of dimethyl sulfoxide solution was added. The intensity of the number of viable cells was measured spectrophotometrically at 570 nm.

### **Formulation and evaluation of gel**

#### ***Preparation of chitosan hydrogel***

Chitosan was dissolved in a 5% (v/v) aqueous acetic acid solution and glutaraldehyde was mixed with chitosan solution stirred at 350 rpm for 1 min and left for 24 h at room temperature. Then, the pH was adjusted to six using sodium hydroxide.<sup>[6,15]</sup>

The Mup-AgNP-Col formulation was gently added to the chitosan hydrogel at a concentration of 5 mg/g and stirred for 5 min.

#### **Evaluation of nanoparticle gel**

##### ***pH of the gel***

The pH of the prepared gel solution was measured by digital pH meter.

##### ***Viscosity***

The rheology of the developed gel was determined by Brookfield viscometer. The spindle type-S64 was used and the angular velocity was increased from 5 to 100 rpm.<sup>[16]</sup>

##### ***Spreadability***

The spreadability of the gel was determined by Texture Analyzer. Calibration was done and the upper cone probe moves toward the sample holder and then the spreadability was measured.

##### ***Extrudability***

100 g of gel was loaded into the load cell of Texture Analyzer. The compression force was applied moving at a speed of 1 mm/s with a force of 10 g.

#### ***In vitro drug release studies***

Exactly 2 g of the sample was placed in a dialysis bag in a beaker containing 200 mL of phosphate buffer pH 7.4 and stirred continuously at 100 rpm. Samples were withdrawn at regular intervals and replenished with appropriate buffers. Samples were then examined in UV visible spectrophotometer for absorbance at 222 nm.

#### ***Drug release kinetics***

Drug release kinetics was estimated using DD solver considering different kinetic models such as zero order, first-order, Higuchi model, Hixson-Crowell model, Korsmeyer-peppas model, and Weibull model. The best-fit model was confirmed by correlation coefficient that was close to 1.<sup>[17]</sup>

### stability studies

To investigate the formulation stability, particle size and zeta potential are measured. The optimized formulation was kept in stability chamber, room temperature and refrigerated temperature, and evaluated at 0, 1, and 2 months.

### Statistical analysis

Particle size, Zeta potential, and *in vitro* release studies were analyzed in triplicate and were expressed as mean  $\pm$  standard deviation of three separate experiments. The results were considered statistically significant when  $P < 0.05$ . Data were evaluated by “one-way ANOVA” performed using GraphPad Prism Software.

## RESULTS AND DISCUSSION

### Extraction and characterization of collagen

#### Collagen yield

The collagen yield from tilapia fish scales was found to be 12.5% of the total fish weight. Collagen yield from tilapia fish scales was reported to be 3.2% by Chen *et al.*<sup>[7]</sup> The yield observed for the species in this study is significantly moderate, indicating that collagen extraction could be commercially viable.

#### Melting point

The melting point of collagen was found to be 78°C which complies with standard values.

#### UV spectroscopy

The lambda max of the collagen was determined as 243 nm [Figure 1].

#### SEM analysis

The freeze-dried collagen shows homogeneous, multi-layered fibrous structure which may be beneficial during cell adhesion and proliferation [Figure 2].

#### FTIR for collagen

The characteristic peaks read for C=C stretching at 1654.98 cm<sup>-1</sup>, N-O Symmetric stretching at 1535.39 cm<sup>-1</sup>, and O-H stretching at 1421.58 cm<sup>-1</sup> confirms the presence of collagen [Figure 3].

#### DoE for silver nanoparticles optimization

Using Design expert software, 2<sup>3</sup> factorial designs eight formulations were formulated to find the good criteria for the synthesis of Mupirocin-loaded AgNps with collagen from

Table 1, the formulation with a lower concentration of silver nitrate, sodium borohydride, and collagen have desirable particle size and drug release. Whereas, the formulation (F6) with a low concentration of silver nitrate and high concentration of sodium borohydride and collagen was found to have desirable entrapment efficacy that is above 94%.

Numerical optimization study was performed for desirability using a second-order regression equation.

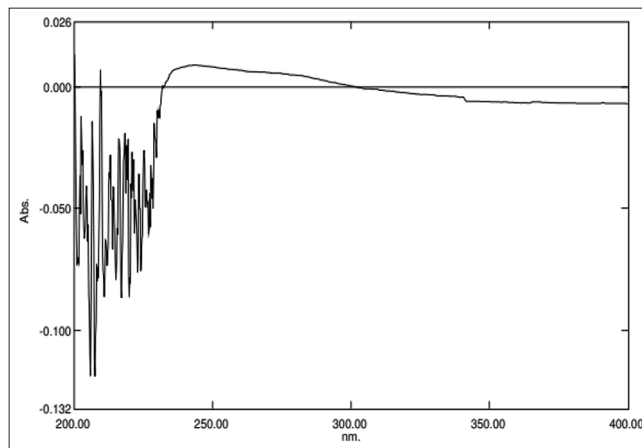


Figure 1: UV spectroscopy of extracted collagen

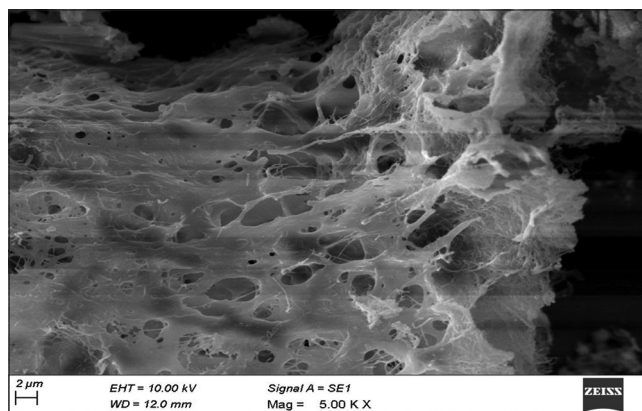


Figure 2: SEM analysis of extracted collagen

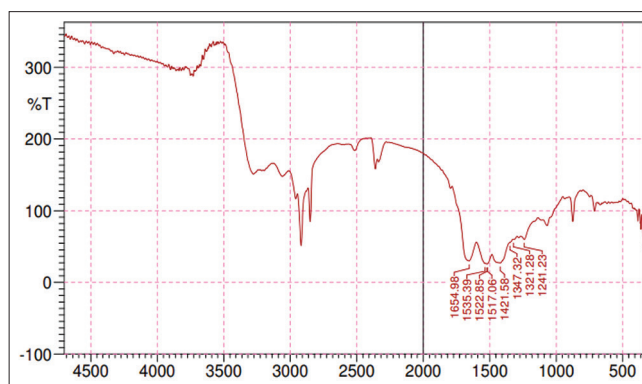


Figure 3: FT-IR data of extracted collagen

**Table 1:** Composition of silver nanoparticle response with dependent variables

Runs	Silver nitrate (mm)	Sodium borohydride (mm)	Collagen (mg)	Particle size (nm)	Entrapment (%)	<i>In vitro</i> drug release (%)
1	5	10	0.5	145.03±1	91.4±0.92	93.2±0.72 at 6 h
2	5	10	0.1	216.2±0.9	92±1	92.8±1.11 at 6 h
3	5	2	0.5	179±0.95	92.8±0.72	91.8±0.80 at 6 h
4	1	10	0.1	186.4±0.5	92.6±0.70	92.5±1.36 at 6 h
5	1	2	0.5	205±2	93.5±0.45	93±1 at 6 h
6	1	10	0.5	173.4±1.5	94.06±0.60	92±2 at 6 h
7	5	2	0.1	128.8±1.8	91±2	91±2.6 at 6 h
8	1	2	0.1	72.27±2.5	92.2±1.05	93.6±1.02 at 6 h

nm is nanometer, h is an hour. Results are shown as mean±SD ( $n=3$ )

The polynomial equation for particle size is

$$Y1 \text{ (Particle Size)} = +162.82+3.68A+16.86B+12.01C-17.46AC-33.58BC$$

Positive values have a synergistic effect while negative values have an antagonistic effect, where “A” is silver nitrate concentration, “B” is sodium borohydride concentration, and “C” is collagen concentration. Increase in  $\text{AgNO}_3$ ,  $\text{NaBH}_4$ , and collagen has a beneficial impact on particle size.

The polynomial equation for drug entrapment efficiency is

$$Y2 \text{ (Entrapment efficiency)} = 92.47-1A+1.18C$$

Increase in silver nitrate has a negative impact on entrapment, but increase in Collagen concentration has a favorable influence on entrapment efficiency.

The polynomial equation for drug release is

$$Y3 \text{ (Drug Release)} = +92.40-0.7500A+0.65B+0.1C+1.0AB+0.75AC$$

Increase in silver nitrate concentration has a detrimental impact on drug release but increases in sodium borohydride and collagen has a favorable influence on drug release.

For the optimized formulation formulated with silver nitrate concentrations of 4.3 mM, sodium borohydride concentration of 2 mM, and collagen concentration of 0.1 mg was found to have an overall desirability value of 0.911 [Figure 4].

The observed particle size according to DoE was 118 nm, but the size predicted was  $121.26 \pm 0.64$  nm, which showed a percentage deviation of 3.3%. For entrapment efficiency, the observed value was 91.3%, the predicted value was  $91.7 \pm 0.6\%$ , and the % deviation was calculated to be 0.5%. The percentage deviation of 1.36% was obtained for *in vitro* release, where the observed value was 91% and the predicted value was  $92.2 \pm 1.10\%$  in 6 h as shown in Figure 4.

### UV spectroscopic analysis

A single robust and wide SPR peak at  $420 \pm 1$  nm was found in the UV visible spectrum as shown in Figure 5 for the optimized formulation confirming the synthesis of AgNPs.

### Characterization of silver nanoparticles

#### DLS

The particle size was determined using Malvern zeta sizer. The optimized Mup-AgNP-col resulted in the average particle size of  $121.26 \pm 0.64$  nm with moderate polydispersion  $0.464 \pm 0.02$ . The zeta potential indicates electrostatic charge as well as the long-term stability. The optimized batches had a zeta potential in the range of  $-21.03 \pm 1$  mV. The particle size and zeta potential were found to be 411 nm and  $-15.1$  mV by Vashishth and Kaushik *et al.*, using trisodium citrate as a reducing agent.<sup>[17]</sup> The particle size and zeta potential are comparatively lower in this study. The decrease could be related to the combination of collagen and the reducing agent, sodium borohydride.

#### Entrapment efficiency

The optimized formulation has a  $91.7 \pm 0.6\%$  entrapment rate. The entrapment efficiency was found to be 67% by Vashishth and Kaushik *et al.*,<sup>[17]</sup> The entrapment was significant in F6 formulation. This may be due to high amount of sodium borohydride and collagen in the formulation. The entrapment was statistically significant according to “one-way ANOVA” ( $P < 0.05$ ).

#### *In vitro* drug release studies

The optimized formulation had a drug release rate of  $92.26 \pm 1.10\%$  in 6 h. The *in vitro* drug release was found to be 97% by Vashishth and Kaushik.<sup>[17]</sup> The graphical representation of optimized formulation is shown in Figure 6. Even though the entrapment is significant, *in vitro* release for the formulations not shown any significant impact when compared to the other formulations.

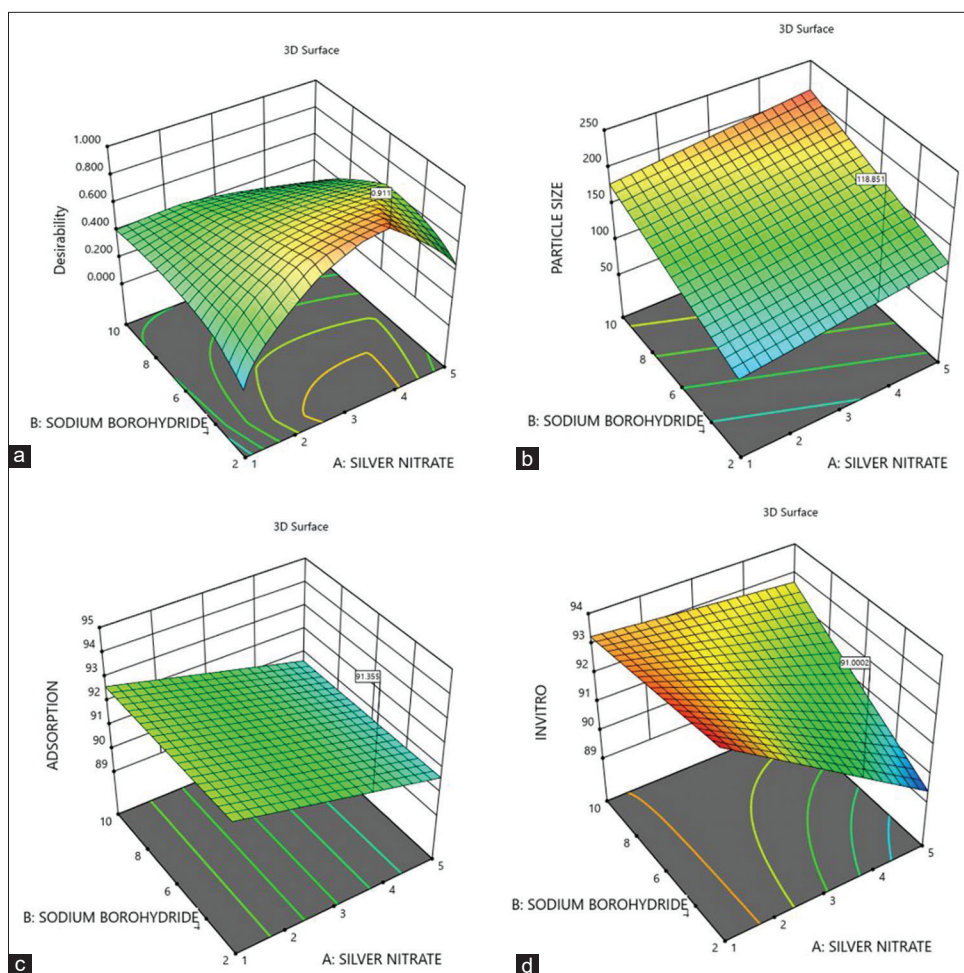


**Figure 4:** 3D surface plot of (a) desirability and its response surface shows effect of X1, X2, and X3 on (b) particle size Y1, (c) entrapment efficiency Y2, and (d) *in vitro* drug release

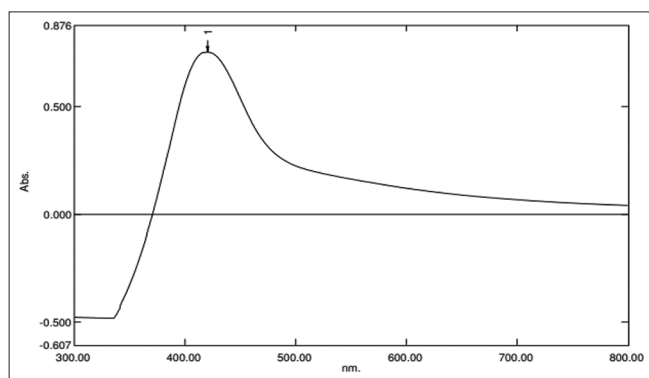


**Figure 5:** UV spectroscopy of optimized formulation

### Atomic force microscopic analysis

AFM was used to visualize morphological characteristics of the optimized nanoparticle. The average height and diameter of polymeric nanoparticles were found to be 56.6 nm and 60 nm. The average height and diameter did not differ much, which shows that the particle is almost spherical. Mup-AgNP-Col's Root mean square and average roughness were evaluated to be 14 and 10 nm. These morphological characteristics revealed that the nanoparticles were rough.

These polymeric nanoparticles surface skewness and surface kurtosis were found to be 0.49 and 1.64 as shown in Figure 7.

### Compatibility studies

FT-IR Data of Physical Mixture (Mup-AgNP Col-NaBH<sub>4</sub>)

The characteristic peaks were read without any major changes with O-H stretching 3295.49cm<sup>-1</sup>, C=O stretching 1715.74cm<sup>-1</sup> for Mupirocin and collagen. Na stretching 891.14 cm<sup>-1</sup> for sodium borohydride observed in the FTIR spectrum of the physical mixture confirms that there is no incompatibility found between the drug and excipients as shown in Figure 8.

### Zone of inhibition

A zone of inhibition is the area was antimicrobial agents come out from the disc and prevents bacterial growth by forming a clear zone around the test product. The zone of inhibition of Mupirocin, Mup-AgNP-Col, and AgNP-Col has been determined. When compared with MRSA, *S. aureus* strain was found to have increased zone of inhibition which states the presence of high antimicrobial activity as shown in Figures 9a and b. The positive control used was Ciprofloxacin as shown in Table 2. When compared statistically

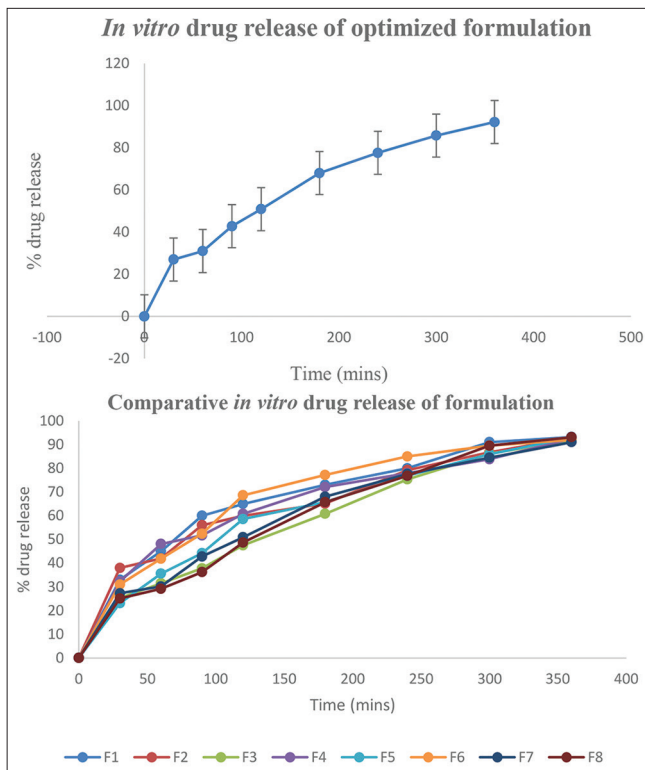


Figure 6: In vitro drug release studies of the optimized formulation and comparative graph of the formulations

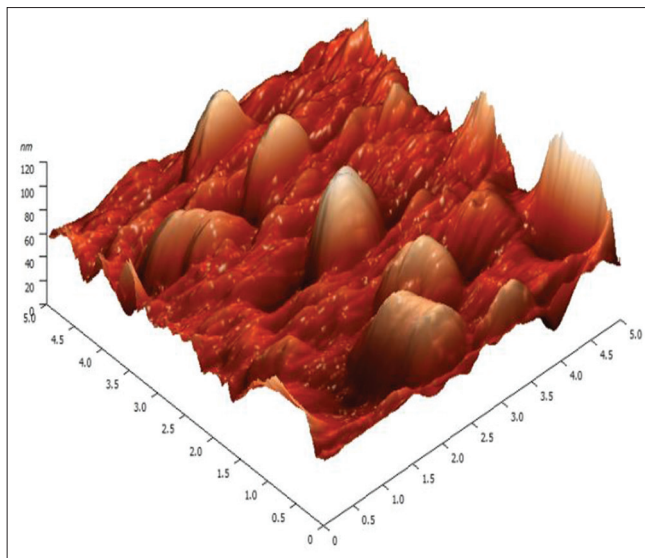


Figure 7: AFM3D images of optimized formulation

*S. auerus* shows more significant antimicrobial action than MRSA according to “Student’s *t*-test” ( $P < 0.001$ ).

**In vitro scratch assay**

The distance of each scratch closure was measured from 0 h to 24 h. The given sample Mup-AgNP-Col synthesized by extracted collagen showed that 87% of wound-healing activity in L929 cells after 24 h is shown in Figure 10 whereas Mup-AgNP-Col prepared by commercial egg collagen showed

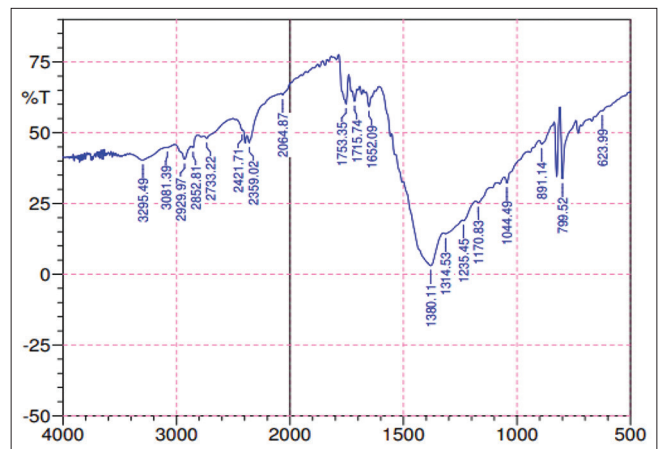


Figure 8: FTIR spectra of physical mixture (Mup-AgNP-NaBH4-Col)

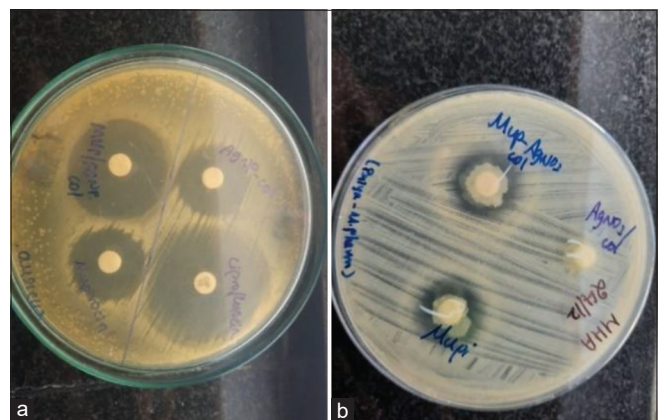


Figure 9: Zone of inhibition (a) Zone of inhibition against *Staphylococcus aureus* (b) Zone of inhibition against MRSA

**Table 2: Zone of inhibition of optimized formulation against *S. aureus* and MRSA**

Antimicrobial agents	Zone diameter (mm) against <i>S. aureus</i>
Mupirocin	30±1
Mup-AgNP-Col	30.6±0.4
AgNP-Col	28±0.7
Ciprofloxacin	35±0.5
Antimicrobial agents	Zone diameter (mm) against MRSA
Mupirocin	28±0.5
Mup-AgNP-Col	25±0.31
AgNP-Col	No zone

mm is millimeter. Results are shown as mean±SD (n=3)

only 50% wound-healing activity after 24 h by Sankar *et al.*<sup>[11]</sup> Restoration of the full cellular density of the mesothelium in fibroblast cells was faster in the Mup-AgNP-Col group than the control group. Mup-AgNP-Col promoted the migration rate of fibroblasts obviously at each time point which was confirmed through the scratch cell distance closure.

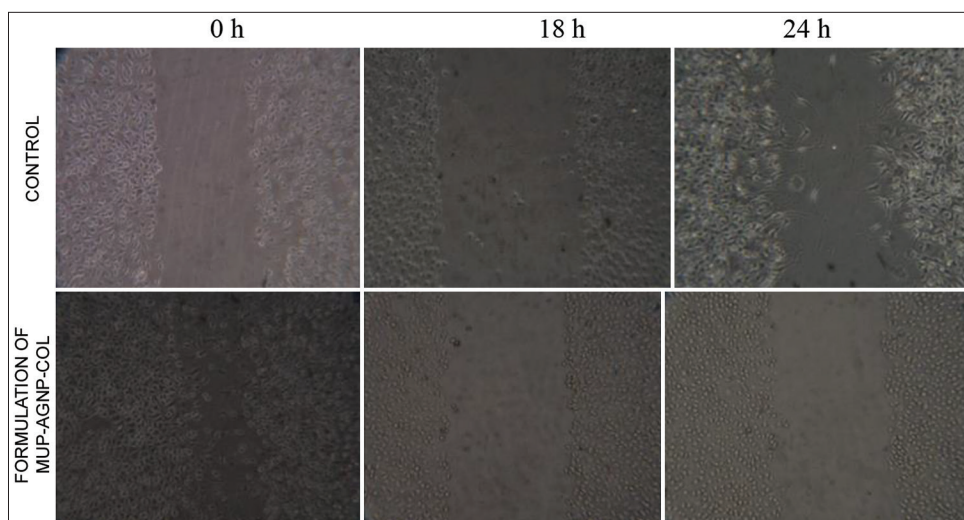


**Figure 10:** *In vitro* scratch assay images of control and Mup-AgNP-Col

### ***In vitro* cytotoxicity studies**

The results suggest that the Mup-AgNP with the collagen was effectively cell proliferative in nature on fibroblasts with increased percentage cell viability values on dose-dependent manner after the incubation period of 24 h. Mup-AgNP-Col shows 99.96% cell viability at 200  $\mu\text{g}$  as shown in Figure 11. The percentage cell viability of Mupirocin solution shows 85% cell at 1024  $\mu\text{g}$  by Golmohammadi *et al.*,<sup>[18]</sup>. Observed results concluded that Mup-AgNP-Col was cell proliferative and it may be due to the presence of cell attachment, protein collagen plays an evident role in fibroblast growth. Significant viability was observed between the untreated and treated according to the “one-way ANOVA” ( $P < 0.0001$ ).

### **Formulation and evaluation of chitosan hydrogel**

#### ***Physical properties of the gel***

The gel was brownish in appearance and smooth to touch, non-gritty, homogeneous in appearance, and there was no sign of phase separation found.

#### ***pH***

The pH of the chitosan gel was found to be neutral that is  $7 \pm 01$ . This means that the chitosan gel can be applied over the skin without causing any skin irritation.

#### ***Viscosity of the gel***

Viscosity is a material’s rheological property which influence its flow properties, viscosity of the gel was found to be 94700 Cp at 20 rpm determined using Brooke field viscometer with spindle number 64 as shown in Table 3.

#### ***Spreadability and extrudability***

The firmness and work of shear denote the ability of the gel to spread over the skin. The firmness and work of shear are indicated by the positive peak and stickiness is indicated

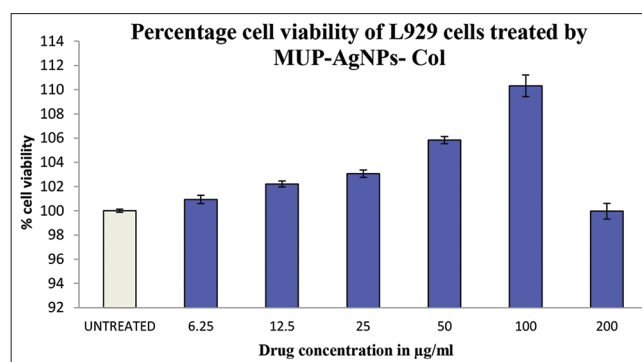


**Figure 11:** % cell viability of L929 Fibroblast cells treated by Mup-AgNPs-Col on various concentrations

**Table 3:** Viscosity, spreadability, and extrudability of hydrogel

Parameters	Obtained value
Viscosity	94700
Spreadability	
Firmness	102 g
Work of shear	110 g/s
Extrudability	859 g

by the negative peak. The firmness and work of shear were found to be 102 g and 110 g/s as shown in Table 3. The force required to extrude the gel from a container is denoted by extrudability which was found to be 859 g in Table 3.

### ***In vitro drug release studies***

The drug release from the chitosan gel was found to be  $86.86 \pm 0.77\%$  and it is represented in graph as shown in Figure 12. This difference was statistically significant according to the Student’s *t*-test ( $P < 0.001$ ) when comparing marketed 2% Mupirocin cream with optimized chitosan hydrogel loaded with silver nanoparticles. About 2%



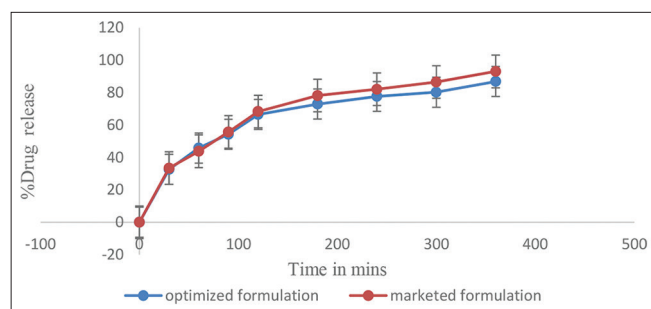


**Figure 12:** *In vitro* drug release studies of optimized hydrogel and marketed 2% Mupirocin cream

**Table 4:** Stability data of the optimized formulation

Months	Temperature conditions	Particle size (nm)	Zeta potential (mV)
0	Room temperature	120±1	-21.2±0.72
	Refrigerated temperature	121.2±1.23	-21.3±0.70
	Stability chamber	122.4±1.21	-21.4±0.75
1	Room temperature	124.6±0.52	-23±0.94
	Refrigerated temperature	125.9±0.95	-23.2±1.07
	Stability chamber	128.6±1.52	-25.2±1.05
2	Room temperature	126.7±0.3	-26.3±0.98
	Refrigerated temperature	127.3±0.81	-24.1±0.6
	Stability chamber	131.1±0.76	-27.03±0.95

nm is nanometer, mV is millivolt. Results are shown as mean±SD ( $n=3$ )

Mupirocin cream showed 93% release in 6 h, whereas optimized formulation showed 86.86±0.77% in 6 h.

### Drug release kinetics

The drug release from the gel can be identified using DD solver. Considering  $r^2$  values, it can be concluded that the Weibull model was the most appropriate with regression coefficient value of 0.9908.

### Stability studies

The optimized formulation was stored at room temperature ( $25 \pm 1^\circ\text{C}$ ), refrigerated temperature ( $8 \pm 1^\circ\text{C}$ ), and in stability chamber ( $40 \pm 1^\circ\text{C}$ ). The particle size and zeta potential of the formulations were measured at 1 and 2 months and compared. In optimized formulation, the percentage deviation of 5% was observed for room temperature, 5% for refrigerated temperature, and 7% for storage in stability chamber. Due

to the less variation in particle size and zeta potential, the formulation stored at room and refrigerated temperature has a better stability than the formulation stored in stability chamber as shown in Table 4.

## CONCLUSION

In this research, collagen was isolated from the scales of a tilapia fish. We utilized DoE software to optimize different parameters. Silver nanoparticles were synthesized by chemical reduction method with collagen which showed significant bactericidal activity on *S. aureus*. According to *in vitro* cytotoxicity the formulation was found to be non-toxic to L929 fibroblast with 99.9% cell viability. *In vitro* scratch assay for Mup-AgNP-Col formulation showed 87% wound closure activity. In this study synthesized, Mup-AgNP-Col multi-composite chitosan hydrogel proven to be an excellent wound-healing material for burn wound infection which provides to have added advantage over marketed cream in its spreadability as well durability and further investigations are warranted to establish the effect on wound closure rate. Investigations with animal models should be performed to establish the *in vivo* efficacy and safety of the developed Mup-AgNP-Col formulation.

## ACKNOWLEDGMENT

We are thankful to PSG College of Pharmacy for providing me with needed facilities and continuous support throughout. We thank The Tamil Nadu Pharmaceutical Science Welfare Trust Chennai, for providing minor project research grand.

## REFERENCES

- Ladhani HA, Yowler CJ, Claridge JA. Burn wound colonization, infection, and sepsis. *Surg Infect (Larchmt)* 2021;22:44-8.
- Konop M, Damps T, Misicka A, Rudnicka L. Certain aspects of silver and silver nanoparticles in wound care: A minireview. *J Nanomater* 2016;1:47.
- Cardoso VS, de Carvalho Filgueiras M, Dutra YM, Teles RH, de Araújo AR, Primo FL, *et al.* Collagen-based silver nanoparticles: Study on cell viability, skin permeation, and swelling inhibition. *Mater Sci Eng C Mater Biol Appl* 2017;74:382-8.
- Kifer D, Muzinic V, Klaric MS. Antimicrobial potency of single and combined mupirocin and monoterpenes, thymol, menthol and 1,8-cineole against *Staphylococcus aureus* planktonic and biofilm growth. *JAntibiot (Tokyo)* 2016;69:689-96.
- Dai T, Tanaka M, Huang YY, Hamblin MR. Chitosan preparations for wounds and burns: Antimicrobial and wound-healing effects. *Expert Rev Anti Infect Ther* 2011;9:857-79.

6. Rohindra DR, Nand AV, Khurma JR. Swelling properties of chitosan hydrogels. *S Pac J Nat Appl Sci* 2004;22:32-5.
7. Chen J, Li L, Yi R, Xu N, Gao R, Hong B. Extraction and characterization of acid-soluble collagen from scales and skin of tilapia (*Oreochromis niloticus*). *LWT Food Sci Technol* 2016;66:453-9.
8. Shalaby M, Agwa M, Saeed H, Khedr SM, Morsy O, El-Demellawy MA. Fish scale collagen preparation, characterization and its application in wound healing. *J Polym Environ* 2020;28:166-78.
9. Chowdhury S, Yusof F, Faruck MO, Sulaiman N. Process optimization of silver nanoparticle synthesis using response surface methodology. *Procedia Eng* 2016;148:992-9.
10. Soorash A, Kwon H, Taylor R, Pietrantonio P, Pine M, Sayes CM. Surface functionalization of silver nanoparticles: Novel applications for insect vector control. *ACS Appl Mater Interfaces* 2011;3:3779-87.
11. Sankar V, Roselin RB, Bhaskar RV. Formulation development of mupirocin adsorbed collagen stabilized silver nanoparticles to enhance synergistic wound healing activity. *J Pharm Sci Res* 2020;12:469-74.
12. Yerragopu PS, Hiregoudar S, Nidoni U, Ramappa KT, Sreenivas AG, Doddagoudar SR. Chemical synthesis of silver nanoparticles using tri-sodium citrate, stability study and their characterization. *Int Res J Pure Appl Chem* 2020;21:37-50.
13. Kaplan O, Tosun NG, Ozgur A, Tayhan SE, Bilgin S, Türkekul I, *et al.* Microwave-assisted green synthesis of silver nanoparticles using crude extracts of *Boletus edulis* and *Coriolus versicolor*: Characterization, anticancer, antimicrobial and wound healing activities. *J Drug Deliv Sci Technol* 2021;64:41-8.
14. Fronza M, Heinzmann B, Hamburger M, Laufer S, Merfort I. Determination of the wound healing effect of *Calendula* extracts using the scratch assay with 3T3 fibroblasts. *J Ethnopharmacol* 2009;126:463-7.
15. Sampath UT, Ching YC, Chuah CH, Singh R, Lin PC. Preparation and characterization of nanocellulose reinforced semi-interpenetrating polymer network of chitosan hydrogel. *Cellulose* 2017;24:2215-28.
16. Patel R, Patel H, Baria A. Formulation and evaluation of Carbopol gel containing liposomes of ketoconazole. (Part-II). *Int J Drug Deliv Technol* 2009;1:42-5.
17. Vashishth V, Kaushik D. Mupirocin amalgamated inorganic nanoparticles for augmenting drug delivery in resistant microbial strains. *World J Pharm Pharm Sci* 2017:1214-29.
18. Golmohammadi R, Najari-Peerayeh S, Moghadam TT, Hosseini SM. Synergistic antibacterial activity and wound healing properties of selenium-chitosan-mupirocin nano hybrid system: An *in vivo* study on rat diabetic *Staphylococcus aureus* wound infection model. *Sci Rep* 2020;10:2854.

**Source of Support:** Nil. **Conflicts of Interest:** None declared.